Diblock Copolymers with a Charged Block in a Selective Solvent: Micellar Structure

Nadezhda P. Shusharina, Irina A. Nyrkova, and Alexei R. Khokhlov*

Physics Department, Moscow State University, Moscow 117234, Russia

Received October 24, 1995; Revised Manuscript Received January 17, 1996[⊗]

ABSTRACT: The structure of the micelles formed by a diblock copolymer with one neutral and one polyelectrolyte block dissolved in highly selective aqueous solutions is studied by the scaling method. In this case an insoluble neutral block forms the core of the micelle, while the corona consists of stretched polyelectrolyte chains. It is taken into account that the corona region can partially lose some of the counterions which can go to the outer solution; therefore the corona is always slightly charged. In some regimes the corona consists of two layers: the inner layer with the concentration blob structure and the outer layer with the electrostatic blob structure. The diagram of states showing different regimes of behavior of the micelles is constructed.

1. Introduction

The formation of micelles and other structures with segregated components in various polymer systems (block copolymers, surfactants, ionomers, associating polymers, etc.) has attracted great interest in recent years.[1−8] Especially, intensive theoretical investigation of these effects was performed (see, e.g., refs 2, 8−13, 15, and 17−19 and the references therein). In particular, it is well-known that in the presence of a selective solvent dilute solutions of diblock copolymers can form micelles.[1,3−5,10,17,18]

One micelle is usually an aggregate which has a spherical dense core made of an insoluble component and a corona consisting of soluble blocks swollen in the solvent (in sufficiently dilute solutions micelles do not overlap and their interaction can be neglected). Being a part of the block copolymer chain, each outer soluble block is grafted to the core, and thus the micelles resemble star polymers. Theoretical background for the consideration of the behavior of stars has been developed by Daoud and Cotton in ref 20. They constructed a scaling theory for the conformation of chains in stars in dilute solutions by taking into account the radial variation of the monomer concentration. Birshtein and Zhulina[10] applied these results for the case of spherical aggregates (micelles) which are formed in the solutions of diblock copolymers. The equilibrium properties of individual micelles containing two neutral components in a dilute selective solvent has been studied by using the scaling method. In ref 10 the main structural characteristics of the micelle were calculated: the radius of the core, the size of the corona, and the equilibrium aggregation number. This approach also proved to be useful for some other block copolymer systems.[11,12]

In the theories mentioned above[9−13] the case of neutral chains was considered. However, one of the most interesting real systems is the water solution where the soluble block can be charged. This produces additional liability to the system. The structural organization in block copolymers with a charged outer block was considered both theoretically[21] and experimentally.[22−27] It should be emphasized that for such systems we have at least two essential consequences of the existence of the charged groups in the corona blocks. First of all, since some of the counterions go to the outer solution, the uncompensated charges on the corona blocks should appear and they lead to additional stretching of the chains due to Coulombic repulsion. On the other hand, the unhomogeneous distribution of counterions in the system also produces important input into the free energy of the micellar solution. The first theory which paid attention to these two factors in the application to polyelectrolytes grafted to a planar surface (polyelectrolyte brush) was presented in ref 14 by Pincus (see also refs 15 and 16). Scaling relations for the brush in different regimes were analyzed. However, in ref 15 only the case of a planar brush was considered and the problem of micellization was not addressed at all.

The situation with polyelectrolyte chains forming an aggregate of spherical symmetry was discussed later in refs 17−19. Marko and Rabin[17] presented a scaling theory for the critical behavior of the micelles in the solution of diblock copolymers with polyelectrolyte and neutral blocks. They calculated the critical micelle size for the two extreme opposite cases: (1) for the weakly charged polyelectrolytes when there is no condensation of counterions and (2) for the limiting case of strongly charged polyelectrolytes (all monomers are charged) when the polyelectrolyte chains are completely stretched. However, the behavior of counterions for the weakly charged case (complete dissociation from the micelle) was introduced into their theory *a priori*.

Dan and Tirrell also examined the aggregation of diblock copolymers consisting of neutral and polyelectrolyte blocks using the scaling theory.[18] However, they dealt with the case of high salt concentrations, and thus they predicted that critical micelle properties were similar to those of neutral copolymers.

In the paper of Misra et al.[19] the mean field model for spherical polyelectrolyte brushes and stars was developed. The authors obtained the main dependencies of the star size on the number of arms and the charge density. It was shown that there are two characteristic regions in the star corona: in the inner region the local structure is determined by non-Coulombic interactions, while in the outer region the electrostatic interactions dominate, so the structure is very different from the one in neutral systems. Yet, it was assumed that the condition of electroneutrality was valid locally; thus the star was a kind of balloon blown up with the gas of counterions. It is clear that this assumption is not always valid; we will see below that it is important to take into account that some finite

[⊗] Abstract published in *Advance ACS Abstracts,* March 1, 1996.

0024-9297/96/2229-3167$12.00/0

fraction of counterions actually leave the micelles and go to the outer solution. Also it is known that the usage of the mean field approach for the case of a good solvent does not give the exact results.

Thus, the general problem of the micellar structure of diblock copolymers with a polyelectrolyte outer block is still waiting for the complete solution. In this paper we construct a scaling theory for an individual micelle made of such block copolymers dissolved in the extremely selective solvent without added low molecular weight salt. The distribution of counterions in the system will be investigated thoroughly, and the whole region of possible values of the system parameters will be examined. In the next section the basic model is specified. Section 3 deals with the properties of the neutral block copolymer micelles, and section 4, with the charged ones. The results of scaling analysis for the general case of a block copolymer with a charged block of arbitrary charge density are described in section 5. Discussion and conclusions are formulated in the last section.

2. Model

Let us consider a solution of diblock copolymer (N_A monomer units in polyelectrolyte block A and N_B monomer units in neutral block B) in a selective solvent which is good for the A block and extremely poor for the B block. The interfacial tension between completely collapsed B blocks and the solvent (or solution of A links) is denoted as $\gamma k_B T$, where T is the temperature and k_B is the Boltzmann constant. Both blocks are supposed to be geometrically identical and flexible; characteristic link volume $v \sim a^3$, a is the monomer unit size of both blocks. The dielectric constant of the solvent is ϵ; e is the elementary charge. The valency of charged groups in the A block and counterions is unity, and there is no added salt in the solution; thus the large scale electrostatic screening in the system is only due to the counterions. The charge density of the A block is defined by the parameter p, which is the fraction of strongly dissociating monomer units in the A block (other monomer units are neutral). Both the cases of weakly charged ($p \ll 1$) and strongly charged ($p \sim 1$) A block will be included in our consideration. The concentration of the block copolymer will be expressed via the volume fraction Φ of the B blocks in the solution.

At very low concentrations Φ the chains do not aggregate in micelles, but (for a long enough B block) each chain forms a collapsed dense B ball with a swollen charged A tail (Figure 1a). We suppose that the solvent is **extremely selective** for B blocks, i.e. that the B blocks are collapsed and that there is practically no solvent inside the balls (globules) formed by B blocks. For higher concentrations the aggregation process with the formation of micelles takes place (Figure 1b). The problem of the formation of micelles will be considered in detail in a separate publication. In this paper we assume that the polymer concentration is higher than the critical micelle concentration, Φ_{cmc}. Below we will be particularly interested in the calculation of the critical size of an isolated micelle which corresponds to the minimum of the free energy of the micelle per chain. Hence, it is these micelles which dominate in the solution. We will assume that these micelles are composed of a certain number m of block copolymer molecules, the radius of their core being R_B and the width of the corona R_A (see Figure 1b); thus the total radius of the micelle is $R \equiv R_A + R_B$. We asume that the solvent is highly selective; therefore the volume

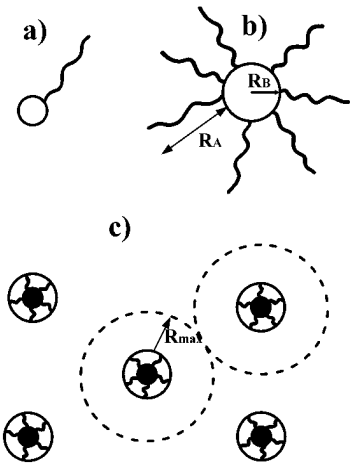

Figure 1. (a) Single block copolymer chain in selective solvent at extremely low concentration $\Phi < \Phi_{cmc}$. (b) Individual micelle consisting of m^* chains. (c) Solution of the micelles.

fraction of B links in the collapsed state is practically unity and, thus,

$$R_B = N_B^{1/3} m^{1/3} a \tag{1}$$

($m = 1$ corresponds to the case of balls, Figure 1a). We will also suppose that the concentration of the solution is so low that the micelles do not overlap, i.e. that $R \ll R_{max}$, where $2R_{max}$ is the average distance between the centers of nearest neighboring micelles in the solution (see Figure 1c), and hence the intermicellear interactions can be neglected. Thus, the following concentration range will be investigated in this paper:

$$\Phi_{cmc} \lesssim \Phi \lesssim \Phi_{max}, \qquad \Phi_{max} \equiv R_B^3/R^3 \tag{2}$$

One more parameter of the system which is necessary to take into account is the degree of dissociation of counterions from the micelles, α. It describes the fraction of the counterions which are outside the micelles, i.e. in the outer solution. The case $\alpha \sim 1$ corresponds to the situation when most of the small ions are floating independently in the solvent around the micelles. In the case $\alpha \ll 1$ most of the counterions are in the "condensed state", i.e. inside the micelles. (Note that this notion of "condensation" has nothing to do with common Onsager−Manning counterion condensation: in the usual sense the dissociation in all the cases under consideration is complete—all chemical groups which can be charged are dissociated.) It turns out that the value of α is very sensitive to the concentration c (see section 4.1).

A similar concept was used in refs 14 and 16 for the case of a planar polyelectrolyte brush. However, in accordance with planar geometry they introduced the length λ which is the spatial size of the cloud of counterions near the charged surface. In our case of spherical geometry and finite concentration Φ the use of the parameter α is more appropriate.

3. Micelles Made of Neutral Block Copolymers ($p \equiv 0$)

We begin here with the case of neutral block copolymers ($p \equiv 0$) which coincides with the one studied by Birshtein and Zhulina.[10] Hence, this section should be regarded mainly as an introduction for the subsequent consideration of a block copolymer with a charged outer block in section 4. However, the calculations of this section are presented in the form which allows direct

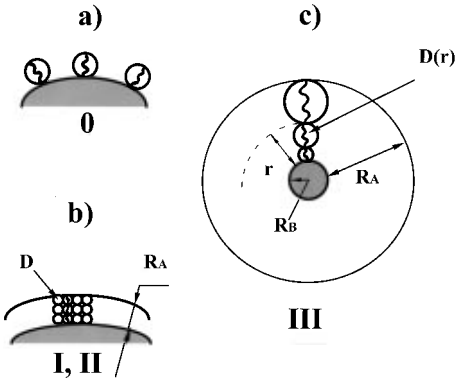

Figure 2. Schematic illustration of three characteristic types of the corona: (a) mushroom structure; (b) planar brush structure ($R_B \gg R_A$); (c) spherical brush structure ($R_A \gg R_B$).

determination of the Φ_{cmc} concentration (which was not available in ref 10): both individual chains and micelles are described in the framework of the same approach.

The free energy per chain of an individual micelle made of m block copolymer chains can be written as a sum of the following contributions (cf. ref 10):

$$\left(\frac{F}{k_BT}\right)_{p\equiv 0} = \frac{F_{core}}{k_BT} + \frac{F_{surf}}{k_BT} + \frac{F_{conc}}{k_BT} + \frac{1}{m}\ln\frac{\Phi}{m} \qquad (3)$$

The first term in eq 3 is the free energy of the core made of blocks B:

$$\frac{F_{core}}{k_BT} \sim \frac{{R_B}^2}{N_B a^2} + \frac{N_B a^2}{{R_B}^2} \sim \frac{m^{2/3}}{{N_B}^{1/3}} + \frac{{N_B}^{1/3}}{m^{2/3}} \qquad (4)$$

In the scaling language this term consists of two contributions: the stretching energy of blocks B (from the Gaussian size $aN_B^{1/2}$ to the size R_B)—it is most important for large enough m—and the compression energy of B blocks into the small globule (is important for $m \sim 1$); cf. refs 28 and 31.

The second term in eq 3 is the surface free energy:

$$\frac{F_{surf}}{k_BT} \sim \gamma\frac{{R_B}^2}{m} \sim \gamma a^2\frac{{N_B}^{2/3}}{m^{1/3}} \qquad (5)$$

For $m \gg 1$ soluble A blocks may be considered as end-grafted chains with grafting density

$$1/\sigma \sim m/{R_B}^2 \sim (m/N_B)^{1/3}a^{-2} \qquad (6)$$

The free energy of this A layer sewed to the A−B interface (the third term in eq 3) can be calculated using the results known from the theory of polymer brushes.[20] Roughly speaking, the free energy of A chains, F_{conc}, is of the order of the number of "concentration blobs" in the corona (in k_BT units)[34]). The following two cases of the geometry of a brush should be distinguished depending on the parameters of the system (see ref 10).

(i) If $R_B \gg R_A$ the outside blocks are sewed to a surface which can be regarded as flat. Hence, in the Alexander−de Gennes brush model language[29] the concentration of monomer units within the brush is constant, and we have the case of a *planar brush*, Figure 2b. The blob size $D \sim g^{3/5}a$, the width of the brush R_A, and the free energy per chain for this case are the following (cf. refs 10 and 20):

$$D \sim \sigma^{1/2} \sim \frac{{N_B}^{1/3}}{m^{1/6}}a \qquad (7)$$

$$R_A \sim \frac{N_A}{g}D \sim \frac{N_A}{{N_B}^{2/9}}m^{1/9}a \simeq R_B\Omega \qquad (8)$$

$$\frac{F_{conc}}{k_BT} \sim \frac{N_A}{g} \sim \frac{N_A}{{N_B}^{5/9}}m^{5/18} \simeq m^{1/2}\Omega \qquad (9)$$

where

$$\Omega \equiv \frac{N_A}{m^{2/9}{N_B}^{5/9}} \qquad (10)$$

The condition $R_B \gg R_A$ is thus equivalent to $\Omega \ll 1$.

(ii) If $R_A \gg R_B$ the concentration of A links falls essentially with the radial coordinate, r. This case may be called a *spherically curved brush*, Figure 2c. The size of the blob increases with r in accordance with the simplest geometric picture (Figure 2c):

$$\frac{D(r)}{D(R_B)} \sim \frac{r}{R_B}; \qquad D(r) \sim ag^{3/5}(r) \qquad (11)$$

The results for this second case are[10,20]

$$\frac{F_{conc}}{k_BT} \sim \int\frac{dr}{D(r)} \sim m^{1/2}\ln\left(\frac{N_A}{m^{2/9}{N_B}^{5/9}}\right) \simeq m^{1/2}\ln\Omega \qquad (12)$$

$$R \simeq R_A \sim \int D(r)\,dr \sim {N_A}^{3/5}m^{1/5}a \simeq R_B\Omega^{3/5} \qquad (13)$$

and the condition $R_A \gg R_B$ is thus equivalent to $\Omega \gg 1$.

However, if the A blocks are very short, they do not interfere at all: the brush has the so-called *mushroom structure* (Figure 2a), and the micelle is described by the following formulas:

$$\frac{F_{conc}}{k_BT} \sim 1, \qquad R_A \sim a{N_A}^{3/5} \qquad (14)$$

This case is also realized if $m \simeq 1$.

From eqs 8, 13, and 14 it follows that the crossover between the planar brush and the spherical brush regimes takes place at $N_A \sim {N_B}^{5/9}m^{2/9}$ (or $\Omega \sim 1$), and between the planar brush and the mushroom structure at $N_A \sim {N_B}^{5/9}/m^{5/18}$ (or $\Omega \sim m^{-1/2}$). Thus, the free energy of the A layer (per chain) can be written as follows (see eqs 9, 12, and 14):

$$\frac{F_{conc}}{k_BT} \sim 1 + m^{1/2}\ln[1+\Omega], \qquad \text{if } m \gg 1 \qquad (15)$$

$$\frac{F_{conc}}{k_BT} \sim 1, \qquad \text{if } m \simeq 1 \qquad (16)$$

Table 1 presents the results of minimization of the free energy (3) with respect to m. They were obtained by Birshtein and Zhulina.[10] The terms which dominate in eq 3 and thus determine the equilibrium value m^* are given in the second column of the table. Usually, the term F_{surf} (5) is in competition with either the first (stretching) part of the term F_{core} (4) (as in regions 0 and I) or the term F_{conc} (15) (in region II with the "planar brush form" of this term, eq 9, and in region III with the "spherical brush form", eq 12).

Table 1. Parameters for the Optimum Neutral Micelles ($p \equiv 0$)

regime	dominant free energy terms	polymer composition	m^*	R_A^*
0	$\frac{F_{core}}{k_BT}+\frac{F_{surf}}{k_BT}$	$N_A < (\gamma a^2)^{-5/18}N_B^{5/18}$	$\gamma a^2 N_B$	$N_A^{3/5}a$
I	$\frac{F_{core}}{k_BT}+\frac{F_{surf}}{k_BT}$	$N_A > (\gamma a^2)^{-5/18}N_B^{5/18}$ $N_A < (\gamma a^2)^{7/18}N_B^{11/18}$	$\gamma a^2 N_B$	$(\gamma a^2)^{1/9}N_A N_B^{-1/9}a$
II	$\frac{F_{surf}}{k_BT}+\frac{F_{conc}}{k_BT}$ (eq 9)	$N_A < (\gamma a^2)^{4/15}N_B^{11/15}$ $N_A > (\gamma a^2)^{7/18}N_B^{11/18}$	$(\gamma a^2)^{18/11}\frac{N_B^{\,2}}{N_A^{\,18/11}}$	$(\gamma a^2)^{2/11}N_A^{9/11}a$
III	$\frac{F_{surf}}{k_BT}+\frac{F_{conc}}{k_BT}$ (eq 12)	$N_A > (\gamma a^2)^{4/15}N_B^{11/15}$	$(\gamma a^2)^{6/5}N_B^{4/5}$	$(\gamma a^2)^{6/25}N_A^{3/5}N_B^{4/25}a$

In region 0 the coils A are grafted onto a planar surface very rarely, so that the coils do not interfere with each other (and so there is only one blob in each chain: $g \sim N_A$, cf. eqs 7, 8, and 14; see Figure 2a. Note that the second (compression) part of F_{core} (4) can come into play only for $m < N_B^{1/2}$, which is possible for $\gamma a^2 N_B^{1/2} \lesssim 1$ (see the value of m^* in Table 1); however, for the case of interest to us (strong segregation limit) this inequality is not valid.

In regime I the corona of the micelle consists of densely packed concentration blobs of size $D \simeq$ const, eq 7 (planar brush, Figure 2b); however the corona is still very thin and hence the size of the micelle is still determined by the term F_{core} (4). The crossover between regions 0 and I takes place at the point $\sigma^{1/2} \sim aN^{3/5}$ or $N_B \sim \gamma a^2 N_A^{18/5}$; see eqs 7 and 14.

Regime II is also the regime of planar geometry for the A blocks (Figure 2b), but as the length of the outer block is larger than for region I, the micellar structure is now determined by a competition of F_{conc} (eq 9) and F_{surf}.

In regime II at fixed N_B the core size R_B^* and the aggregation number m^* decrease with increasing N_A, whereas the corona width R_A^* increases. Finally, the corona width becomes of the order of the core size, and we enter regime III, where the curvature of the corona becomes apparent; see Figure 2c. As F_{conc} specified by eq 12 only logarithmically depends on N_A, the power dependence of critical parameters m^* and R_B^* on N_A disappears.

Using the approach described in this section, we can also find the critical micelle concentration Φ_{cmc}. At the point of micellization there is equilibrium between the micelles of critical size m^* and lone chains (micelles with $m = 1$, Figure 1a), the concentration of these lone chains is just Φ_{cmc} (cf. with the definitions of Φ_{cmc} in refs 17 and 18). As $m^* \gg 1$ (see Table 1), the corresponding condition of equilibrium can be written as follows

$$\Phi_{cmc} \simeq \exp\left[\frac{E_{m^*} - E_1}{k_BT}\right] \tag{17}$$

where

$$\frac{E_m}{k_BT} = \left(\frac{F(m)}{k_BT}\right)_{p\equiv 0} - \frac{1}{m}\ln\frac{\Phi}{m} \tag{18}$$

and $(F(m)/k_BT)_{p\equiv 0}$ is defined in eq 3. Thus the final result is

$$\Phi_{cmc} = \Phi_0 \exp\left(-N_B^{1/3} - \gamma a^2 N_B^{2/3}\right)\exp\left(\frac{E_{m^*}}{k_BT}\right) \tag{19}$$

where the equilibrium values of m^* are given Table 1.

For the minimization of eq 3 with respect to m the last translational term $m^{-1}\ln\Phi$ is not important provided that $\Phi \gtrsim \Phi_{cmc}$. That is why the concentration Φ does not enter in the final formulas; see Table 1.

4. The Case of Charged Block Copolymers

In this section we will consider the solution of diblock copolymers with polyelectrolyte soluble A blocks. For this case the additional free energy contributions caused by the presence of charges on the chains and the distribution of counterions must be taken into account. The free energy of polyelectrolyte micelle per chain can be written as a sum of the following contributions:

$$\left(\frac{F}{k_BT}\right)_{p\neq 0} = \frac{F_{core}}{k_BT} + \frac{F_{surf}}{k_BT} + \frac{F_{conc}}{k_BT} + \frac{F_{elst}}{k_BT} + \frac{1}{m}\ln\frac{\Phi}{m} \tag{20}$$

where the additional term is

$$\frac{F_{elst}}{k_BT} = \frac{F_{charge}}{k_BT} + \frac{F_{c/i}}{k_BT} \tag{21}$$

The first part here is the electrostatic energy of the outer layer of the micelle due to the presence of charges. The second one is the translational entropy of nonuniformly distributed counterions. The origin of these terms will be considered in detail in section 4.1, where it will be shown that these terms depend essentially on the geometry of the micelle (mostly on its size R). To determine R, one needs to investigate the structure of the corona of the charged micelle in detail; this is done in section 4.2.

4.1. Distribution of Counterions. As seen from eqs 20 and 21 two new free energy terms appear in the case of charged micelles: F_{charge} and $F_{c/i}$. These terms reflect the accounting for two new physical factors: electrostatic energy of the micelle as a charged object and entropic contribution caused by the translational entropy of nonuniformly distributed counterions. To calculate these terms, let us subdivide all the space of the solution into two spatial regions (cf. ref 30). One of these regions corresponds to the space inside the micelles (core + corona); another region is the space outside the micelles. The radius of each micelle is $R = R_A + R_B$; let R_{max} be the average distance between the centers of nearest neighbor micelles (see Figure 1c). In our approximation the inequality $R_{max} \gg R$ is valid (see the condition (2)). The entropy of the distribution of counterions between the two regions can be expressed through the parameter α which is a fraction of counterions in the outer region. Therefore, the free energy

of a charged spherical micelle plus counterions is given by

$$F_{\text{elst}} = \frac{Q^2\alpha^2}{\epsilon R} + k_B T\frac{Q}{e}(1-\alpha)\ln\left(\frac{Q}{e}\frac{(1-\alpha)a^3}{R^3}\right) + k_B T\frac{Q}{e}\alpha\ln\left(\frac{Q}{e}\frac{\alpha a^3}{R_{\max}{}^3}\right) \quad (22)$$

where $Q = N_A pme$ is the total charge of the micelle. (Note that $F_{\text{elst}} \equiv F_{\text{elst}}/m$.) The first term in eq 22 is the electrostatic energy of a charged sphere of radius R. The next two terms are the translational entropy of counterions inside and outside the micelle, respectively. The expression (22) may be rewritten as

$$F_{\text{elst}} = \alpha\left(\frac{Q^2\alpha}{\epsilon R} + k_B T\frac{Q}{e}\ln\left(\frac{Q}{e}\frac{\alpha}{1-\alpha}\frac{R^3}{R_{\max}{}^3}\right)\right) + k_B T\frac{Q}{e}\ln\left(\frac{Q}{e}\frac{(1-\alpha)a^3}{R^3}\right) \quad (23)$$

To obtain the equilibrium distribution of counterions, the value of F_{elst} should be minimized with respect to α. This leads to the following equation:

$$\frac{Q^2\alpha}{\epsilon R} + k_B T\frac{Q}{e}\ln\left(\frac{\alpha}{1-\alpha}\frac{R^3}{R_{\max}{}^3}\right) = 0 \quad (24)$$

Thus from (23) and (24) we obtain for F_{elst}

$$\frac{F_{\text{elst}}}{k_B T} = N_A pm\ln(m(1-\alpha)) \quad (25)$$

From (24) the following estimations for α can be obtained:

$$\alpha = \begin{cases} \frac{1}{z}\ln\frac{1}{\Phi} & \text{if } \alpha \ll 1 \\ 1 - \Phi e^z & \text{if } 1-\alpha \ll 1 \end{cases} \quad (26)$$

$$z \equiv N_A pm\frac{ua}{R} \quad (27)$$

where $u \equiv e^2/\epsilon a k_B T$ is the characteristic dimensionless parameter connected with Coulomb interactions. At ordinary conditions (e is the charge of an electron, $a \sim$ 1 nm, $k_B T \sim$ 300 K, $\epsilon \approx 80$ for water solution) the parameter u is approximately equal to unity.

Limiting cases (26) correspond to the situation when counterions are mainly present either inside the micelle or outside it. The crossover between these regimes is determined by the block copolymer concentration in the solution: at concentration $\Phi > e^{-z}$ counterions "condense" on the micelle; i.e. practically all of them are inside the corona. If the polymer concentration Φ is less than e^{-z}, most of the counterions are outside the micelle freely floating in the solvent. The free energy electrostatic contribution in each of these cases is given by the expressions

$$\frac{F_{\text{elst}}}{k_B T} \equiv \frac{F_{\text{elst}}/m}{k_B T} = \begin{cases} N_A p\ln m + N_A p\frac{1}{z}\ln\Phi & \text{if } \Phi > e^{-z} \\ N_A p\ln m + N_A p\ln\Phi & \text{if } \Phi < e^{-z} \end{cases} \quad (28)$$

It can be seen that the electrostatic contribution (28) consists of two terms: the first one is the same in both concentration regimes, whereas the second one is negative and depends on concentration. Below we will consider only the case $\alpha \ll 1$, i.e. when counterions are mainly trapped within the micelle, which corresponds to the first line in eq 28. In the opposite case ($\alpha \sim 1$) we are facing the problem of the chain of "electrostatic blobs"[34] in the strong electric field of the inner shell of the charged corona. This case needs a more detailed consideration and will be considered in another publication.

Thus the problem is to minimize the free energy (20) with eqs 4, 5, 9, 12, and 28. The second term of the first line in eq 28 has a different form depending on R. The determination of R will be considered in detail in the next section.

4.2. Blob Picture of the Corona. First of all, let us describe a blob picture of the layer of polyelectrolyte A blocks. For neutral chains the blob structure in the brush is essentially similar to one in a three-dimensional semidilute solution.[9,10] However, contrary to neutral systems, polyelectrolyte micelles do not exhibit packing of the blobs.[32,33] The conformation of a charged macromolecule which is affected by Coulomb interactions may be throught of as a sequence of electrostatic blobs. The size of the electrostatic blob, D_{elst}, is determined by the condition that the energy of the electrostatic repulsion of two neighboring blobs along the chain is equal to the thermal energy:

$$\frac{(gp)^2 e^2}{\epsilon D_{\text{elst}}} \sim k_B T \quad (29)$$

where g is the number of links in the blob.[32] The same consideration can be used for the corona structure in the case $\alpha \ll 1$. Besides, in the good solvent

$$D_{\text{elst}} \sim ag^{3/5} \quad (30)$$

Thus for the size of the electrostatic blob we have

$$D_{\text{elst}} \sim u^{-3/7}p^{-6/7}a \quad (31)$$

The free energy of the corona per chain is proportional to the number of blobs per chain:[34]

$$\frac{F_{\text{elst}}}{k_B T} \sim k \sim \frac{N_A}{g} \sim N_A p^{10/7}u^{5/7} \quad (32)$$

As is clear from eq 32 the free energy of electrostatic blobs is independent of m and therefore this contribution does not influence the critical behavior of the micelle.

The thickness of the corona in this regime is equal to the length of the chain of the blobs:

$$R_A \sim kD_{\text{elst}} \sim N_A u^{2/7}p^{4/7}a \quad (33)$$

and the radius of the corona does not depend on the aggregation number. This result has been obtained in the paper of Misra and co-workers[19] by mean field consideration. One can note that the micelle radius for this case is independent of the number of arms and chains are very strongly stretched: $R_A \sim N_A$.

If $R_B \gg R_A$, i.e. for a planar layer, the dense packing of the concentration blobs converts to single electrostatic blob chains (see Figure 3a). In the case of the essential curvature of the B core the blob picture is changed, as is shown in Figure 3b. For very long A blocks there is a spherical layer of blobs. But in the inner layer of the corona we have densely packed blobs, while in the outer layer the stretched electrostatic chains of blobs "grow" from the dense layer of concentration blobs. It is clear that in the regions filled by concentration and electro-

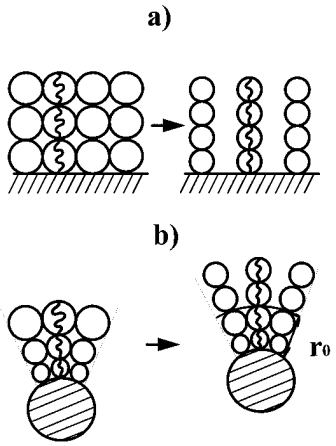

Figure 3. Possible changes in the blob picture of the corona of a polyelectrolyte micelle. (a) A planar brush structure of concentration blobs can be converted to the brush structure of single elongated chains of electrostatic blobs. (b) A spherical brush structure of concentration blobs can be converted to the two-shell structure (concentration blobs in the inner shell, electrostatic blobs in the outer shell.

static blobs the sizes of corresponding blobs coincide. The condition $D_{elst} = D_j$ gives us the expression for r_0 (the distance from the core surface to the first electrostatic blob along the blob chain):

$$R_0 = p^{-6/7} m^{1/2} a \tag{34}$$

Thus for the determination of F_{elst} in eq 28 we obtained the following estimations for R:

$$R \simeq N_B^{1/3} m^{1/3} a \quad \text{in the case of a planar brush} \tag{35}$$

$$R \simeq N_A^{3/5} m^{1/5} a \quad \text{in the case of a spherical brush} \tag{36}$$

$$R \simeq N_A u^{2/7} p^{4/7} a \quad \text{in the case of electrostatic blobs} \tag{37}$$

5. Scaling Analysis and Results

The parameters of the equilibrium micelle in the case $\alpha \ll 1$ can be determined by the minimization of the free energy (see eq 20) with respect to m. F_{elst} is given by the first line of eq 28 with substitutions of eqs 27, 35, 36, and 37; it turns out that the second term of F_{elst} is not important. In Table 2 main parameters for the polyelectrolyte micelles are presented in the form of scaling estimations. The diagram of Figure 4a shows the regimes of different behavior of the micelles depending on polyelectrolyte block length N_A and the charge fraction p (at a fixed length of the insoluble block; N_B = const and γ = const). The boundaries in this diagram correspond to some relations between the system parameters (see Table 2) and do not depend on the concentration of block copolymers in the solution.

Regimes 0−III are the same as for neutral blocks. For these regimes the polyelectrolyte nature of the outer block is of no importance.

Due to the presence of the free energy term F_{elst}/k_BT the new regimes IV and V can be identified. In regime IV A blocks are grafted onto the quasiplanar surface of the core; regime V corresponds to the spherical geometry of the outer layer. The micelle characteristics (size, aggregation number, etc.) for regimes IV and V essentially depend on the degree of charging of the polyelectrolyte block, p.

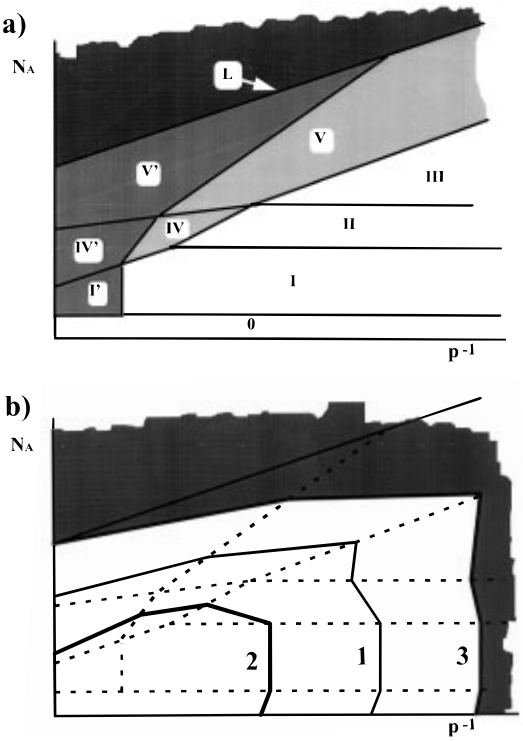

Figure 4. (a) Diagram of possible regimes of behavior of polyelectrolyte micelles in the solution. The micellar structure in each of the regimes I−IV corresponds to one of the schematic pictures in Figure 5. The crossover boundaries of different regimes and micellar characteristics are given in Table 2. For regimes 0−III the electrostatic contributions are not important, while for the shaded regimes and IV and V they determine the micellar structure. In regimes I′, IV′, and V′ there are electrostatic blobs in the micellar corona. Line L corresponds to the aggretation number $m = 1$. Above this line the multimolecular micelles do not exist. (b) Diagram of regimes of Figure 4a with the superimposed crossover lines corresponding to the boundary between the cases when most of counterions are kept inside the micelle or escaped to the external solution. Crossover line for some given value of Φ (curve 1), $\Phi = \Phi_{cmc}$ (curve 2), $\Phi = \Phi_{max}$ (curve 3).

As was shown above, for strongly charged A blocks $D_{elst} < D_{conc}$ and stretched chains of electrostatic blobs appear. All the regimes with electrostatic blobs are designated in Figure 4a with a prime (regimes I′, IV′, and V′). In the case of a quasiplanar core surface (regimes I′ and IV′), instead of the dense packing of concentration blobs we have a number of isolated chains with electrostatic blobs (Figure 3a). In regime V′ the structure of the micellar corona is essentially different: dense packing of concentration blobs takes place only in the inner layer of the corona, up to the radius r_0. At $r > r_0$ there are stretched chains of electrostatic blobs (see Figure 3b). Line L is equivalent to the equation $m = 1$ in the regime V ($N_A = \gamma a^2 N_B^{2/3} p^{-1}$; see Table 2), and therefore above it the micelles do not exist.

Let us now discuss how the diagram in Figure 4a changes with the change of concentration. The case $\alpha \ll 1$ is valid only if some condition depending on Φ is satisfied (see eqs 28 and 27). The diagram for which the concentration dependencies are taken into account is presented in Figure 4b. At a given concentration Φ we can build line 1, which corresponds to the crossover between the cases $\alpha \ll 1$ and $\alpha \sim 1$. This line encircles the area where most of counterions are within the corona of the micelle; outside this area most of the counterions are free. The equations for the curves in different regimes of the diagram of Figure 4a are given by the following expressions:

$$0: \quad N_A = N_B^{-5/2} p^{-5/2} \left(\ln \frac{1}{\Phi}\right)^{5/2} \tag{38}$$

$$I: \quad p^{-1} = N_B^{10/9} \left(\ln \frac{1}{\Phi}\right)^{-1} \tag{39}$$

$$II: \quad N_A = N_B^{11/12} p^{11/16} \left(\ln \frac{1}{\Phi}\right)^{-11/16} \tag{40}$$

$$III: \quad N_A = N_B^{-8/5} p^{-5/2} \left(\ln \frac{1}{\Phi}\right)^{5/2} \tag{41}$$

$$IV: \quad N_A = N_B^{3/4} p^{-5/8} \left(\ln \frac{1}{\Phi}\right)^{-3/8} \tag{42}$$

$$V: \quad N_A = N_B^{4/5} p^{-7/10} \left(\ln \frac{1}{\Phi}\right)^{-1/2} \tag{43}$$

$$IV', V': \quad N_A = N_B^{2/3} p^{-6/7} \left(\ln \frac{1}{\Phi}\right)^{-1/3} \tag{44}$$

In accordance with eq 2 line 1 can "move" across the diagram in the range from $\Phi = \Phi_{cmc}$ to $\Phi = \Phi_{max}$. The critical micelle concentration in the case of charged micelles is determined by eq 19 where m^* for the regimes IV, V, IV′, and V′ is given in Table 2. The crossover line 1 at $\Phi = \Phi_{cmc}$ is plotted as curve 2 in Figure 4b, while this line at $\Phi = \Phi_{max}$ is designated as curve 3. At $\Phi = \Phi_{max}$ the micelles begin to overlap and our approach ceases to be valid.

In Figure 5 we present the schematic pictures of the micelles and the blob picture of the corona for the different regimes. Figure 5a corresponds to regimes I and II, 5b to regimes I′ and IV′, 5c to III and V, 5d to V′, and 5e corresponds to regime 0.

6. Discussion

In the present paper we have considered the equilibrium properties of a dilute solution of diblock copolymers with a polyelectrolyte block at concentrations above the critical micelle concentration. The characteristics for the optimum individual micelle have been obtained in the framework of the scaling approach. The free energy of the system includes the contributions which are important for neutral micelles (see ref 10) and also the new terms which are connected with the polyelectrolyte nature of one of the blocks. To calculate these terms, it was necessary to investigate the influence of counterions and their spatial distribution for the micelles of different sizes. As a result we have constructed the diagram of different regimes of behavior of the micellar solution (Figure 4a); the aggregation numbers m^* for the optimum micelle for each of the regions of the diagram of Figure 4a are given in the Table 2, and the schematic blob pictures of the micellar corona are shown in Figure 5.

Table 2. Parameters for the Optimum Polyelectrolyte Micelles ($p \neq 0$)

regime	dominant free energy terms	polymer composition	m^*	R_A^*	R_B^*
0	$\frac{F_{core}}{k_BT} + \frac{F_{surf}}{k_BT}$	$N_A < N_B^{5/18}$	$\gamma a^2 N_B$	$N_A^{3/5} a$	$(\gamma a^2)^{1/3} N_B^{2/3} a$
I	$\frac{E_{core}}{k_BT} + \frac{F_{surf}}{k_BT}$	$N_A < (\gamma a^2)^{7/18} N_B^{11/18}$ $p > (\gamma a^2)^{-7} N_B^{7/36} u^{1/2}$ $N_A < (\gamma a^2)^{2/3} N_B^{1/3} p^{-1}$ $N_A > N_B^{5/18}$	$\gamma a^2 N_B$	$(\gamma a^2)^{1/9} N_A N_B^{-1/9} a$	$(\gamma a^2)^{1/3} N_B^{2/3} a$
II	$\frac{F_{surf}}{k_BT} + \frac{F_{conc}}{k_BT}$	$N_A < (\gamma a^2)^{4/15} N_B^{11/15}$ $N_A > (\gamma a^2)^{7/18} N_B^{11/18}$ $N_A < (\gamma a^2)^{18/11} p^{-11/5}$	$(\gamma a^2)^{18/11} \frac{N_B^2}{N_A^{18/11}}$	$(\gamma a^2)^{2/11} N_B^{9/11} a$	$(\gamma a^2)^{6/11} \frac{N_B}{N_A^{6/11}} a$
III	$\frac{F_{surf}}{k_BT} + \frac{F_{conc}}{k_BT}$	$N_A > (\gamma a^2)^{4/15} N_B^{11/15}$ $N_A < (\gamma a^2)^{3/5} N_B^{2/5} p^{-1}$	$(\gamma a^2)^{6/5} N_B^{4/5}$	$(\gamma a^2)^{6/25} N_A^{3/5} N_B^{4/25} a$	$(\gamma a^2)^{2/5} N_B^{3/5} a$
IV	$\frac{F_{surf}}{k_BT} + \frac{F_{charge}}{k_BT}$	$N_A > (\gamma a^2)^{2/3} N_B^{1/3} p^{-1}$ $N_A < (\gamma a^2)^{2/5} N_B^{3/5} p^{-2/5}$ $N_A > (\gamma a^2)^{18/11} p^{-11/5}$ $N_A < (\gamma a^2) p^{-19/7} u^{-6/7}$	$(\gamma a^2)^3 \frac{N_B^2}{N_A^3 p^3}$	$(\gamma a^2)^{1/3} N_A^{2/3} p^{-1/3} a$	$(\gamma a^2) \frac{N_B}{N_A p} a$
V	$\frac{F_{surf}}{T} + \frac{F_{charge}}{T}$	$N_A > (\gamma a^2)^{2/5} N_B^{3/5} p^{-2/5}$ $N_A > (\gamma a^2)^{3/5} N_B^{2/5} p^{-1}$ $N_A < (\gamma a^2)^{3/5} N_B^{2/5} p^{-41/35}$	$(\gamma a^2)^3 \frac{N_B^2}{N_A^3 p^3}$	$(\gamma a^2)^{3/5} N_B^{2/5} p^{-3/5} a$	$(\gamma a^2) \frac{N_B}{N_A p}$
I′	$\frac{F_{core}}{k_BT} + \frac{F_{surf}}{k_BT}$	$N_A < (\gamma a^2)^{2/3} N_B^{1/3} p^{-1}$ $p < (\gamma a^2)^{-7} N_B^{7/36} u^{1/2}$ $N_A > N_B^{5/18}$	$\gamma a^2 N_B$	$N_A u^{2/7} p^{4/7} a$	$(\gamma a^2)^{1/3} N_B^{2/3} a$
IV′	$\frac{F_{surf}}{k_BT} + \frac{F_{charge}}{k_BT}$	$N_A > (\gamma a^2)^{2/3} N_B^{1/3} p^{-1}$ $N_A < (\gamma a^2)^{2/5} N_B^{3/5} p^{-2/5}$ $N_A > (\gamma a^2) p^{-19/7} u^{-6/7}$	$(\gamma a^2)^3 \frac{N_B^2}{N_A^3 p^3}$	$N_A u^{2/7} p^{4/7} a$	$(\gamma a^2) \frac{N_B}{N_A p} a$
V′	$\frac{F_{surf}}{k_BT} + \frac{F_{charge}}{k_BT}$	$N_A > (\gamma a^2)^{2/5} N_B^{3/5} p^{-2/5}$ $N_A > (\gamma a^2)^{3/5} N_B^{2/5} p^{-41/35}$	$(\gamma a^2)^3 \frac{N_B^2}{N_A^3 p^3}$	$N_A u^{2/7} p^{4/7} a$	$(\gamma a^2) \frac{N_B}{N_A p} a$

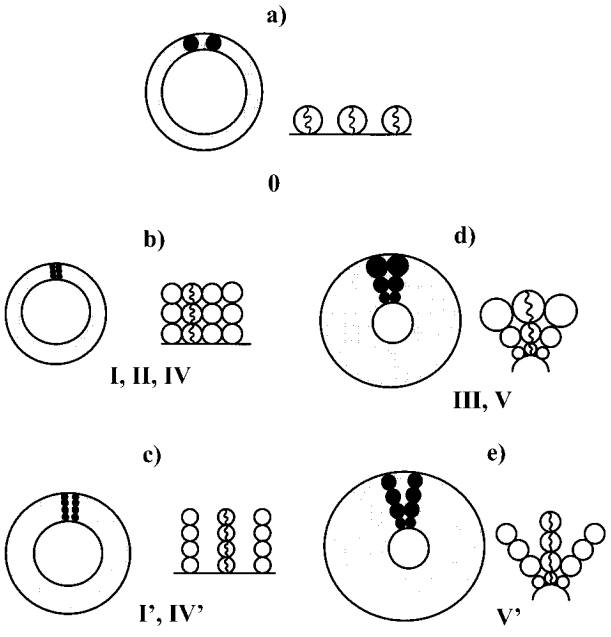

Figure 5. Schematic representation the polyelectrolyte micelle for different regimes: (a) mushroom structure of the corona; (b) corona composed of concentration blobs (planar case); (c) corona composed of electrostatic blobs (planar case); (d) corona composed of concentration blobs (spherical case); (e) corona composed of concentration blobs in the inner shell and electrostatic blobs in the outer shell (spherical case).

Regimes 0, I, II, and II are the same as the ones in Birshtein and Zhulina's paper[10] (see section 2.1). Due to the presence of charges in the outer block new regimes I′, IV′, and V′ appear. The structure of the corona in these regimes is completely different from that known for neutral block copolymers (see section 4); the stretched chains consisting of electrostatic blobs appear instead of the dense packing of concentration blobs. The formulas for the boundaries of the regimes are presented in Table 2.

The diagram in Figure 4a and schematic representation of the micelles in Figure 5 correspond to the case when most of the counterions are inside the micelle $\alpha \ll 1$. (The case $\alpha \sim 1$ will be considered in another publication.) Realization of this condition depends on the total concentration of the solution Φ. In the framework of the two-phase approximation we have analyzed the concentration dependence of the condition $\alpha \ll 1$. The results are illustrated in Figure 4b.

The possibility of different spatial distributions of the counterions depending on the charge density of the polyelectrolyte block was discussed also by Marko and Rabin.[17] In the case of strongly charged chains ($p \sim 1$) our results coincide with the ones of ref 17. However, for the cases $p \lesssim 1$ and $p \ll 1$ the spatial distribution of counterions also essentially depends on Φ and it is necessary to consider both cases $\alpha \sim 1$ and $\alpha \ll 1$. At the same time in ref 17 only the case $\alpha \sim 1$ was considered for weakly charged polymers. As mentioned above, this case requires in fact a more detailed consideration, because electrostatic blobs are subjected to a strong external electric field.

The obtained effect of stretching of the polyelectrolyte block and of separation of the corona in two regions with concentration blobs inside and electrostatic blobs outside (see Figure 3b) is analogous to the result obtained in ref 19, where a similar possibility was discussed in the framework of mean field theory. However, we presented a scaling picture of this effect which clarifies its physical meaning.

Our theory can be used for the formulation of new experimental studies of the aqueous solutions of block copolymers containing a polyelectrolyte and neutral hydrophobic block. Also, the theory can be easily generalized in many respects, and this will be done in subsequent publications. We already mentioned the problem of the regimes corresponding to $\alpha \sim 1$. The influence of added low molecular weight salt is another important question. Finally, we have considered in more detail the process of the formation of micelles at the cmc and have calculated the micellar size distributions below and above the cmc[35] (while in the present study we limited the analysis to optimum size micelles).

Acknowledgment. We are grateful to the Russian Foundation for Basic Research and the International Science Foundation for financial support.

References and Notes

(1) *Developments in Block Copolymers*; Goodman, I., Ed.; Applied Science: New York, 1982 (Vol. 1), 1985 (Vol. 2).
(2) Israelachvili, J. N. *Intermolecular and Surface Forces with Applications to Colloidal and Biological Systems*; Academic Press Inc. Ltd.: London, 1985.
(3) *Processing, Structure and Properties of Block-Copolymers*; Folkes, M. J., Ed.; Elsevier: New York, 1985.
(4) *Block Copolymers: Science and Technology*; Meier, D. J., Ed.; MMI Press/Harwood Academic Publishers: New York, 1983.
(5) *Polymeric Surfactants*; Piirma, I., Ed.; Marcel Dekker: New York, 1992.
(6) *Structure and Properties in Ionomers*; Pinery, M., Eisenberg, A., Ed.; NATO Advanced Study Institute Series 198; D. Reidel Publishing Co.: Dordrecht, Holland, 1987.
(7) *Multiphase Polymers: Blends and Ionomers*; Utracki, L. A., Weiss, R. A., Eds.; ACS Symposium Series 395; American Chemical Society: Washington, DC, 1989.
(8) Semenov, A. N.; Nyrkova, I. A.; Khokhlov, A. R. Statistics and Dynamics of Ionomer Systems. In *Ionomers: Properties and Applications*; Schlick, S., Ed.; CRC Press: Boca Raton, FL, 1996.
(9) Zhulina, E. B., Birshtein, T. M. *Vysokomol. Soedin. A* **1985**, *27*, 511.
(10) Birshtein, T. M.; Zhulina, E. B. *Polymer* **1989**, *30*, 170.
(11) Fredrickson, G. H.; Leibler, L. *Macromolecules* **1989**, 422, 1238.
(12) Halperin, A. *Macromolecules* **1991**, *24*, 1418.
(13) Semenov, A. N. *Macromolecules* **1993**, *26*, 2273.
(14) Pincus, P. *Macromolecules* **1991**, *24*, 2912.
(15) Borisov, O. V.; Birshtein, T. M.; Zhulina, E. B. *J. Phys. II* **1991**, *1*, 521.
(16) Wittmer, J.; Foanny, J. F. *Macromolecules* **1993**, *26*, 2691.
(17) Marko, J. F.; Rabin, Y. *Macromolecules* **1992**, *25*, 1503.
(18) Dan, N.; Tirrell, M. *Macromolecules* **1993**, *26*, 4310.
(19) Misra, S.; Mattice, W. L.; Napper, D. H. *Macromolecules* **1994**, *27*, 7090.
(20) Daoud, M.; Cotton, J. P. *J. Phys.* **1982**, *43*, 531.
(21) Zhulina, E. B. *Macromolecules* **1993**, *26*, 6273.
(22) Wu, G.; Zhou, Z.; Chu, B. *Macromolecules* **1993**, *26*, 2117.
(23) Astafieva, I.; Zhong, X. Fu; Eisenberg, A. *Macromolecules* **1993**, *26*, 7339.
(24) Khougaz, K.; Gao, Zh.; Eisenberg, A. *Macromolecules* **1994**, *27*, 6341.
(25) Selb, J.; Gallot, Y. *Macromol. Chem.* **1981**, *181*, 1491.
(26) Selb, J.; Gallot, Y. *Macromol. Chem.* **1981**, *181*, 1513.
(27) Valint, P. L.; Bock, J. *Macromolecules* **1988**, *21*, 175.
(28) Birshtein, T. M.; Pryamitsyn, V. A. *Polym. Sci. USSR* **1987**, *29*, 2039; *Macromolecules* **1991**, *24*, 1554.
(29) Alexander, S. *J. Phys. (Paris)* **1977**, *38*, 983.
(30) Oosawa, F. *Polyelectrolytes*; M. Dekker: New York, 1970.
(31) Grosberg, A. Yu.; Khokhlov, A. R. *Statistical Physics of Macromolecules*; American Institute of Physics: NY, 1994.
(32) De Gennes, P. G.; Pincus, P.; Velasco, R. M.; Brochard, F. *J. Phys.* **1976**, *37*, 1461.
(33) Khokhlov, A. R.; Khachaturian, K. A. *Polymer* **1982**, *23*, 1742.
(34) de Gennes, P.-G. *Scaling Concepts in Polymer Physics*; Cornell University Press: Ithaca, NY, 1979.
(35) Shusharina, N. P.; Saphonov, M. V.; Nyrkova, I. A.; Khalatur, P. G.; Khokhlov, A. R. *Ber. Bunsen-Ges. Phys. Chem.*, to be published.

MA9515745